

## Electronic Supplementary Information (ESI)

### **Coordinated Water Molecules Induced Solid-State Superprotonic Conduction by a Highly Scalable and pH-Stable Coordination Polymer (CP)**

Rupam Sahoo,<sup>a†</sup> Shaozhen Luo,<sup>b†</sup> Naresh Kumar Pendyala,<sup>b†</sup> Santanu Chand,<sup>a</sup> Zhi-Hua Fu,<sup>b</sup> and Madhab C. Das<sup>a\*</sup>

<sup>a</sup>Department of Chemistry, Indian Institute of Technology Kharagpur, Kharagpur 721302, WB, India.

E-mail: [mcdas@chem.iitkgp.ac.in](mailto:mcdas@chem.iitkgp.ac.in)

<sup>b</sup>State Key Laboratory of Structural Chemistry, Fujian Institute of Research on the Structure of Matter, Chinese Academy of Sciences (CAS), 155 Yangqiao Road West, Fuzhou, Fujian, 350002 (China)

† These authors contributed equally to this work.

---

### Table of Contents

	Experimental section	S2-S4
<b>Figure S1</b>	Optical photograph and single crystal image of <b>IITKGP-101</b>	S4
<b>Figure S2</b>	Asymmetric unit of <b>IITKGP-101</b>	S5
<b>Figure S3</b>	$\pi \cdots \pi$ stacking interactions in <b>IITKGP-101</b>	S5
<b>Figure S4-S5</b>	H-bonding interactions in <b>IITKGP-101</b>	S6
<b>Figure S6-S7</b>	Laboratory atmosphere exposed PXRD and FT-IR plot	S7
<b>Figure S8-S9</b>	TGA and DSC plots of <b>IITKGP-101</b>	S8
<b>Figure S10-S11</b>	VTPXRD plot, EDX mapping, FESEM image of <b>IITKGP-101</b>	S9
<b>Figure S12</b>	Humidity treated PXRD plot of <b>IITKGP-101</b>	S10
<b>Figure S13</b>	Images of proton conduction measurement setup for <b>IITKGP-101</b>	S10
<b>Figure S14-S15</b>	Humidity-dependent proton conductivity plots of <b>IITKGP-101</b> in single crystal form	S11
<b>Figure S16</b>	Water sorption isotherm for <b>IITKGP-101</b>	S12
<b>Figure S17</b>	Humidity-dependent proton conductivity plots of <b>IITKGP-101</b> in pellet form	S12
<b>Figure S18</b>	Optical photograph of <b>IITKGP-101</b> device and anhydrous condition Nyquist plots of <b>IITKGP-101</b>	S12
<b>Figure S19</b>	Activation energy plot of <b>IITKGP-101</b>	S13
<b>Figure S20</b>	PXRD comparison after impedance measurement	S13
<b>Table S1-S4</b>	Crystallographic Data	S14-S16
<b>Table S5-S6</b>	Proton conduction results summary of <b>IITKGP-101</b>	S16-S17
<b>Table S7-S8</b>	Proton-conductivity comparison tables	S17-S18
	References	S19

**Materials and reagents.** Copper(II) Nitrate Hexahydrate ( $\text{Cu}(\text{NO}_3)_2 \cdot 6\text{H}_2\text{O}$ , CAS #: 13478-38-1, Merck), Disodium 2,6-Naphthalenedisulfonate (Molecular Formula:  $\text{C}_{10}\text{H}_6\text{Na}_2\text{O}_6\text{S}_2$ , CAS #: 605-70-9, TCI), 4,4'-Bipyridine (Molecular Formula:  $\text{C}_{10}\text{H}_8\text{N}_2$ , CAS #: 553-26-4, Alfa Aesar), Ammonia solution 25 % ( $\text{NH}_4\text{OH}$ , CAS #: 1336-21-6, Merck). All reagents were obtained from commercial sources and used without further purification.

**Physical Measurements.** The FT-IR spectra were recorded in the range of 400-4000  $\text{cm}^{-1}$  on a Perkin-Elmer RX1 spectrophotometer. PXRD patterns were recorded using  $\text{Cu-K}_\alpha$  radiation (1.5418 Å) on a Bruker D8 Advance diffractometer. The variable temperature powder X-ray diffraction (VTPXRD) study was recorded using Spring 8 (BL02B2) with  $\lambda = 0.63\text{Å}$ . Thermogravimetric analysis (TGA) was performed using a TG 209 F3 Tarsus (Netzsch), and the sample was heated from room temperature to 800 °C at a rate of 5 °C  $\text{min}^{-1}$  under  $\text{N}_2$  atmosphere. Differential scanning calorimetry (DSC) was performed using Perkin Elmer Pyris Diamond DSC under the  $\text{N}_2$  atmosphere. SEM image of **IITKGP-101** CP: The morphology of as-synthesized single crystals of **IITKGP-101** CP was observed by CarlZeiss MERLIN field-emission scanning electron microscopy (FESEM, JSM 6700F) at an acceleration voltage of 15 kV.

**Synthesis of IITKGP-101.** A mixture of 0.024 g  $\text{Cu}(\text{NO}_3)_2 \cdot 6\text{H}_2\text{O}$  (0.1 mmol), 0.033 g disodium 2,6-Naphthalenedisulfonate ( $\text{NDSNa}_2$ , 0.1 mmol) and 0.008 g 4,4'-Bipyridine (0.05 mmol) were dissolved in 5 mL deionized water. The resulting solution was stirred at room temperature for 15 min and after that,  $\text{NH}_4\text{OH}$  was added dropwise until the solution became clear. The clear solution was stirred for another 30 min, filtered, and the filtrate was kept for crystallization at ambient temperature. Blue block shaped crystals suitable for single crystal X-ray diffraction were collected by filtration after 5 days. The crystals were rinsed with distilled water and dried in the air, giving a yield of 78% based on  $\text{Cu}(\text{NO}_3)_2 \cdot 6\text{H}_2\text{O}$ . Elemental analysis calculated for  $\text{C}_{40}\text{H}_{54}\text{Cu}_4\text{N}_4\text{O}_{29}\text{S}_4$ : C, 33.42; H, 3.78; N, 3.89; S, 8.92; found: C, 33.24; H, 3.44; N, 3.84; S, 8.17.

**G-scale Synthesis of IITKGP-101.** A mixture of  $\text{Cu}(\text{NO}_3)_2 \cdot 6\text{H}_2\text{O}$  (1 mmol, 0.241 g), disodium 2,6-Naphthalenedisulfonate (1 mmol, 0.332 g), 4,4'-Bipyridine (0.5 mmol, 0.078 g) were dissolved in 30 ml deionized water and  $\text{NH}_4\text{OH}$  was added dropwise in the stirring condition until the solution became clear. After that, the clear solution was filtered and the filtrate was kept for crystallization at ambient temperature. After 5 days, the blue crystals were collected by filtration.

### Crystallographic Data and Structure Refinements:

Good quality single crystal of **IITKGP-101** was sorted out with the help of a polarizing microscope and immersed in paratone oil, which was then mounted on the tip of glass fiber and cemented using epoxy resin. The single-crystal XRD diffraction data were collected at 100 K on a Bruker AXS (D8 Quest System) X-ray diffractometer, equipped with a PHOTON 100 CMOS detector using graphite-monochromated Mo- $K_{\alpha}$  radiation (0.71073 Å). The linear absorption coefficients, scattering factors for the atoms, and the anomalous dispersion corrections were taken from International Tables for X-ray Crystallography. Bruker Apex III software was used for data collection, unit cell measurements, absorption corrections, scaling, and integration.<sup>1,2</sup> The data were reduced and an empirical absorption correction was applied with the help of SAINTPLUS software and SADABS programs using XPREP, respectively.<sup>3,4</sup> The structures were solved by the direct method using SHELXL-2014 in the WinGx programs. The WinGx package of programs was used to carry out the full-matrix least-squares refinement against the function  $|F^2|$ .<sup>5,6</sup> For all the cases, non-hydrogen atoms were refined anisotropically. All other hydrogen atoms were geometrically fixed using the riding atom model and assigned fixed isotropic displacement parameters. It should be noted that several attempts to fix the actual positions of the hydrogens in  $\text{Cu}_4(\mu_3\text{-OH})_4$  SBUs was unsuccessful. The “ACTA” command was used to generate the Crystallographic Information File (CIF). The structural details of all the compounds are presented in **Table S1**. CCDC: **2220922** contain the crystallographic data for **IITKGP-101**. These data are available from The Cambridge Crystallographic Data Center (CCDC) via [www.ccdc.cam.ac.uk/data\\_request/cif](http://www.ccdc.cam.ac.uk/data_request/cif).

**Water sorption measurement details.** Water sorption isotherm was carried out on an automated micropore gas analyzer BELSORP-max (Microtrac BEL Corp.). Before the sorption measurement, the sample was activated at 100 °C under vacuum ( $10^{-3}$  Pa) for 10 h. The water vapor isotherms were measured at each equilibrium pressure by the static volumetric method at 298 K under  $P/P_0 = 0.85$ .

**Proton conduction Analysis.** Proton conductivity measurements were performed using a quasi-four-electrode AC impedance technique with a Solartron 1260 impedance/gain-phase analyzer. The microcrystalline samples were compressed to 0.71 mm in thickness and 2.5 mm in diameter under a pressure of  $\sim 0.1$  GPa. Two sides of the pellet were connected to gold wires using gold

paste. For single-crystal measurements, crystal sizes were determined by indexing the crystals of **IITKGP-101** on a Rigaku Pilatus CCD diffractometer. Gold wires were connected to both ends of the longer axis of each crystal (**Figure S12**). The sample pellet and single crystals were both measured at frequencies ranging from  $10^7$  to 0.1 Hz as the temperatures were varied from 30 to 80 °C and/or as the relative humidities (RH) were varied from 40 to 98%. The conductivity of the samples was deduced from the Debye semicircle in the Nyquist plot.

The activation energy ( $E_a$ ) for the materials was estimated from the following equation:

$$\sigma T = \sigma_0 \exp(-E_a/k_b T)$$

where  $\sigma$  is the proton conductivity,  $\sigma_0$  is the pre-exponential factor,  $k_b$  is the Boltzmann constant, and T is the temperature.

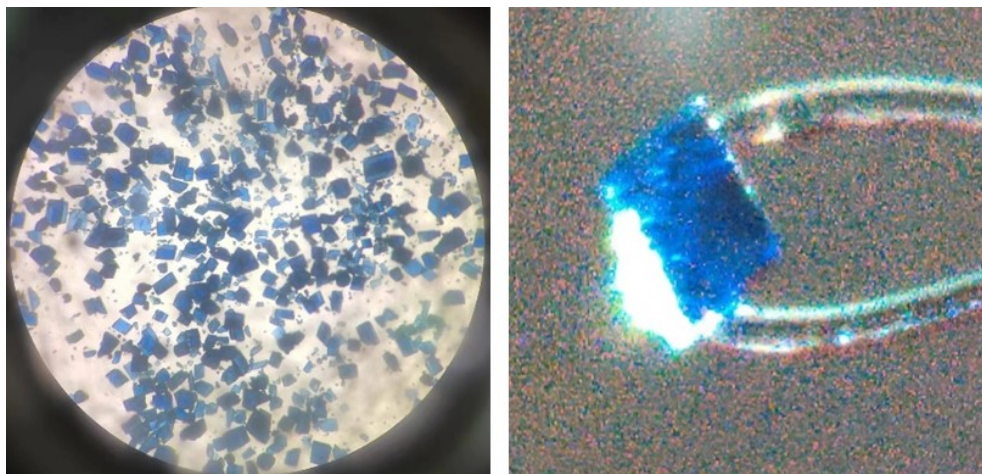


**Figure S1:** Optical photograph and single crystal image of **IITKGP-101**.

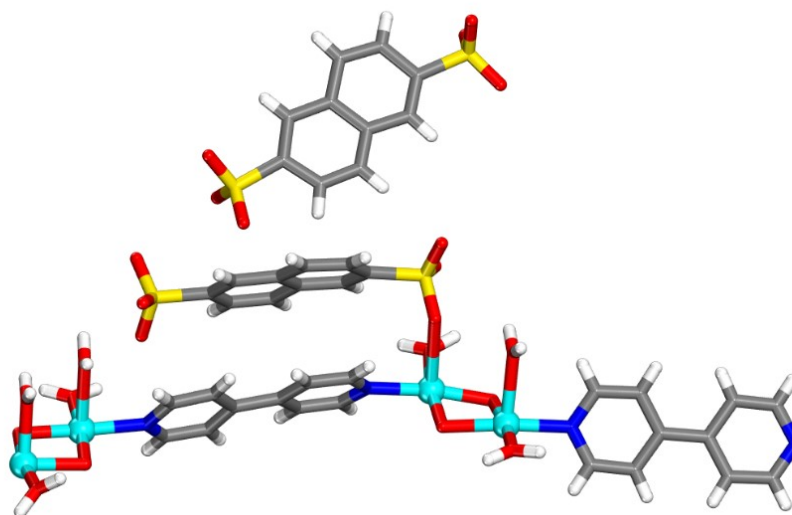


**Figure S2:** Asymmetric unit of **IITKGP-101** (Color codes: Cu, cyan; O, red; S, yellow; N, blue; C, gray; H, white). Lattice water molecules were removed for clarity reason.

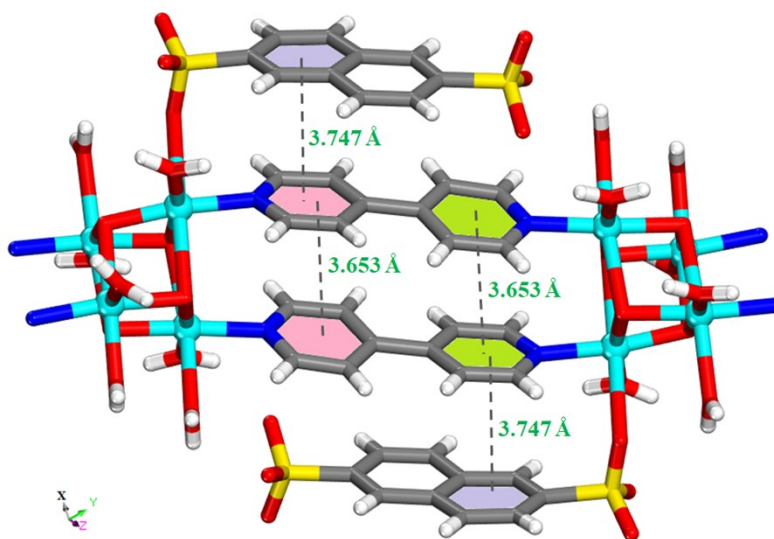


**Figure S3:**  $\pi \cdots \pi$  stacking interactions in **IITKGP-101** (Color codes: Cu, cyan; O, red; S, yellow; N, blue; C, gray; H, white).

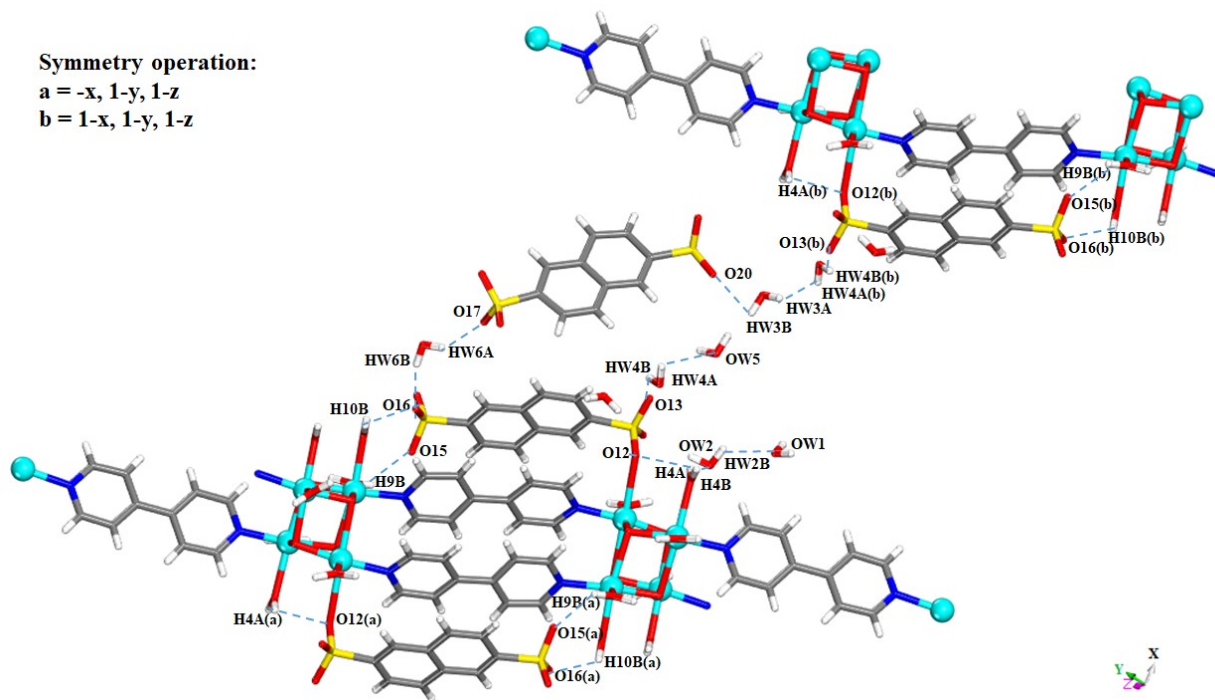


**Figure S4:** Extended H-bonding interactions present in **IITKGP-101** (Color codes: Cu, cyan; O, red; S, yellow; N, blue; C, gray; H, white).

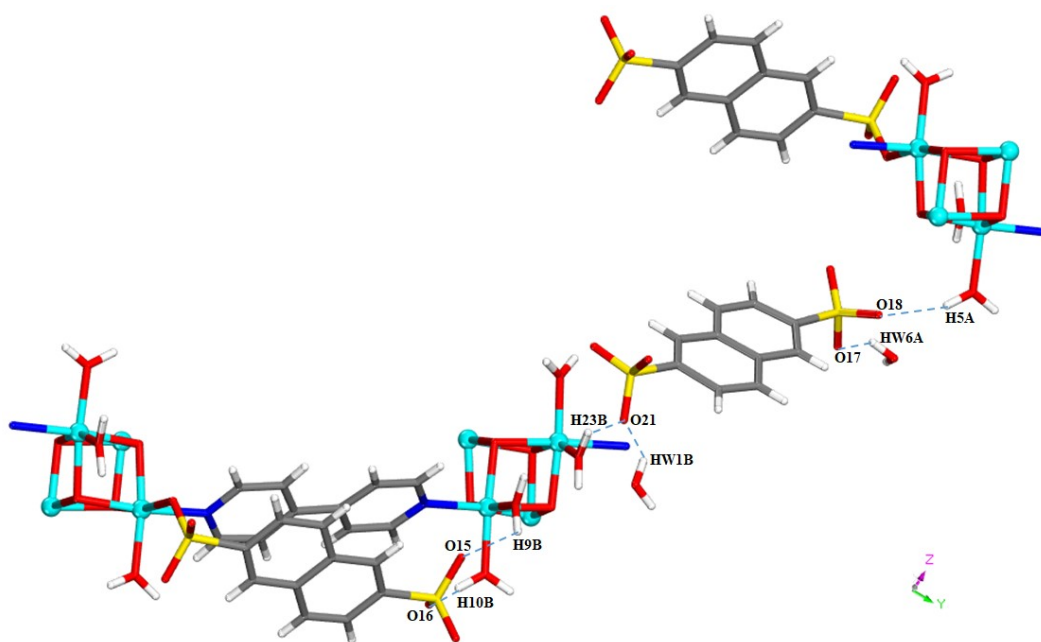


**Figure S5:** A portion of H-bonding interaction displaying lattice 2,6-NDS units connected two different 1D chains *via* H-bonding (Color codes: Cu, cyan; O, red; S, yellow; N, blue; C, gray; H, white).

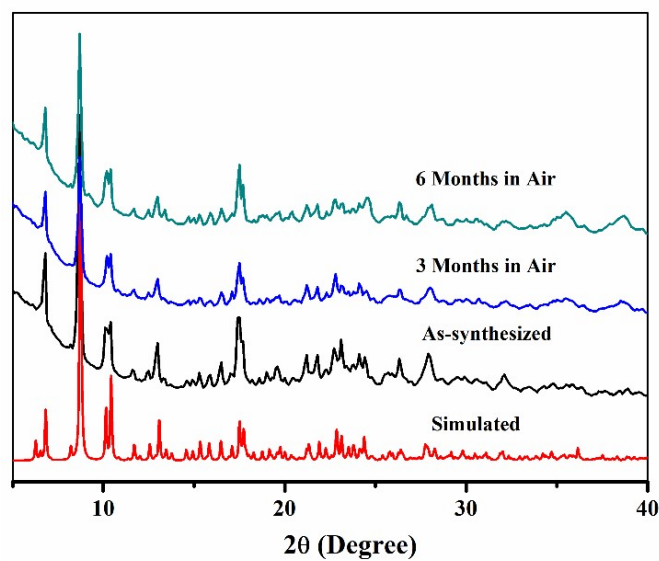


**Figure S6:** PXRD pattern of IITKGP-101 after exposing in laboratory atmosphere.

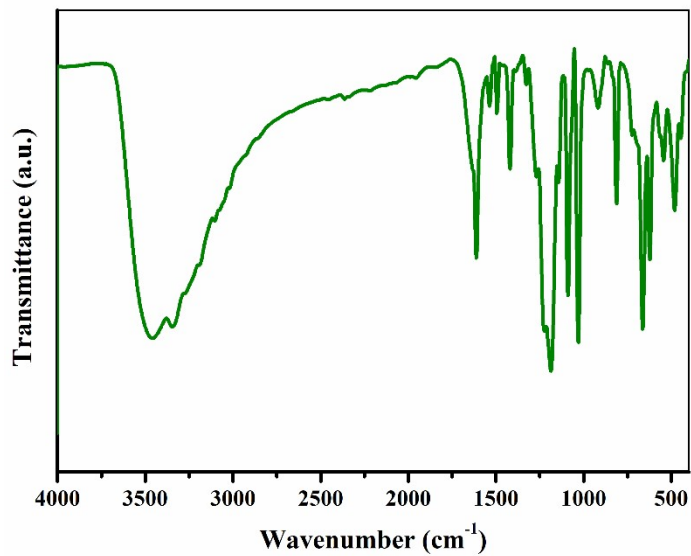


**Figure S7:** FT-IR spectra of IITKGP-101 at room temperature. The broad and strong peak from 3500 to 3000  $\text{cm}^{-1}$  assigned to water molecules.

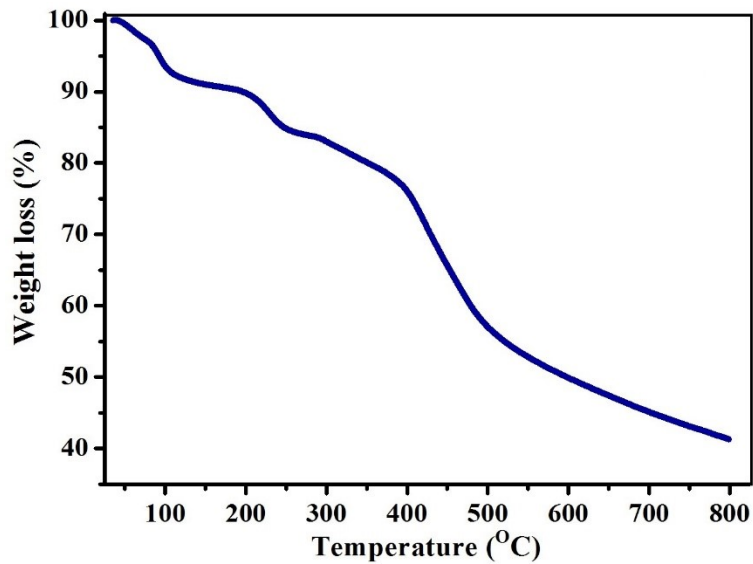


Figure S8: TGA plot of as-synthesized IITKGP-101.

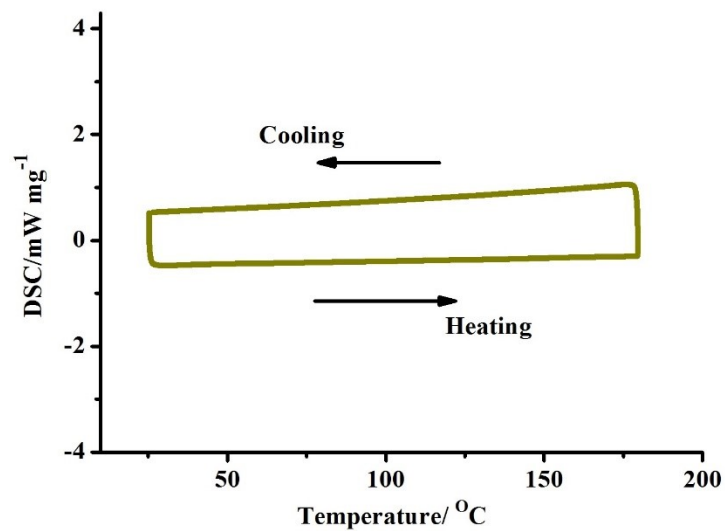
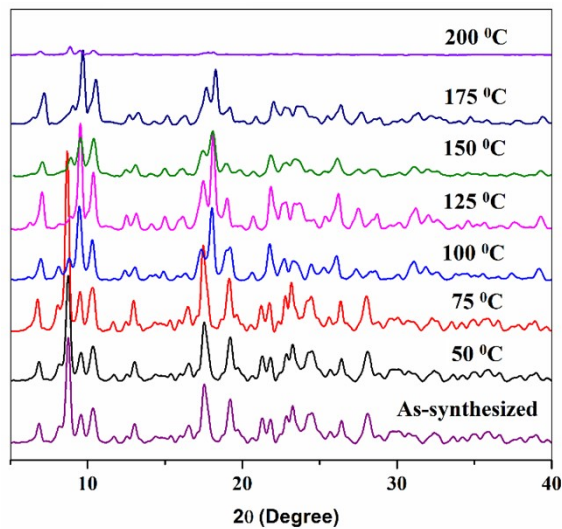
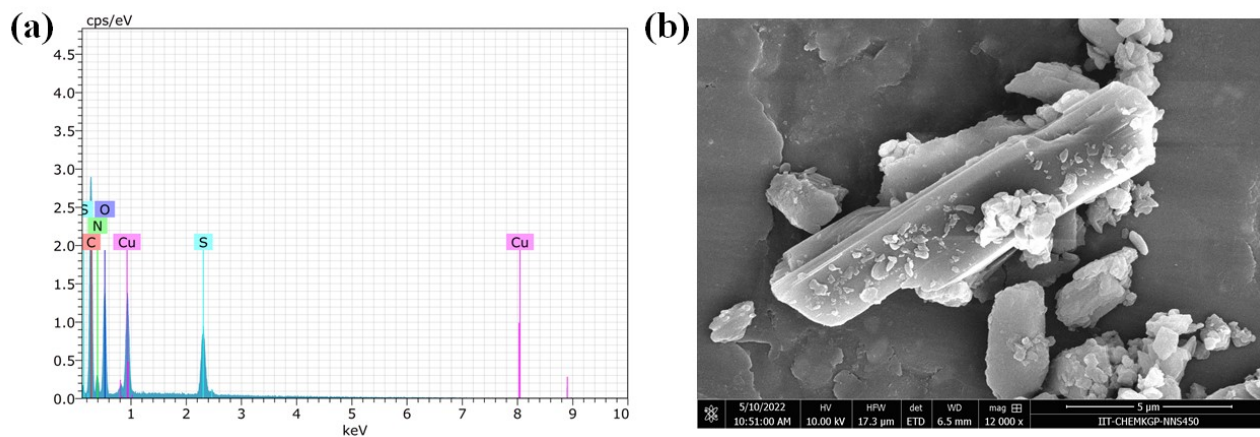


Figure S9: Differential scanning calorimetric plot for IITKGP-101.





**Figure S10:** Variable temperature PXRD patterns for IITKGP-101 ( $\lambda = 0.63\text{\AA}$ ).



**Figure S11:** (a) EDX mapping of IITKGP-101 showing the absence of  $\text{Na}^+$ ; (b) FESEM image of IITKGP-101 showing the crystalline nature.

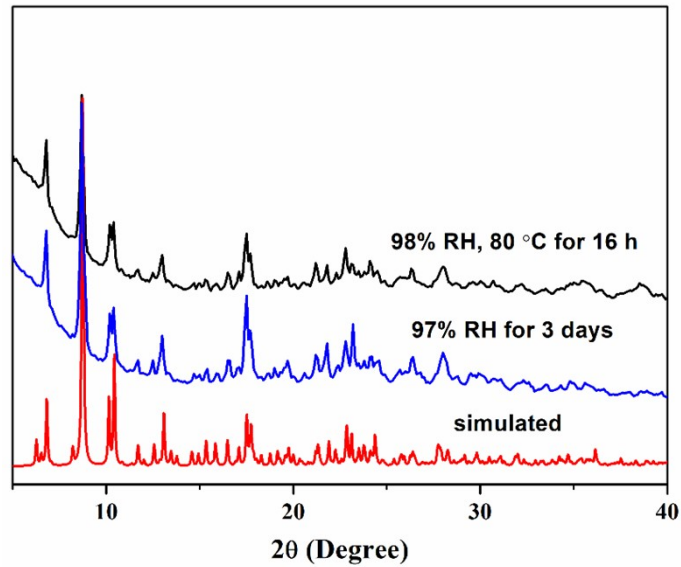


**Figure S12:** PXRD comparison of simulated **IITKGP-101** (red), after 97% RH test for 3 days (blue) and after exposure to 98% RH and 80 °C simultaneously for 16 hours (black).

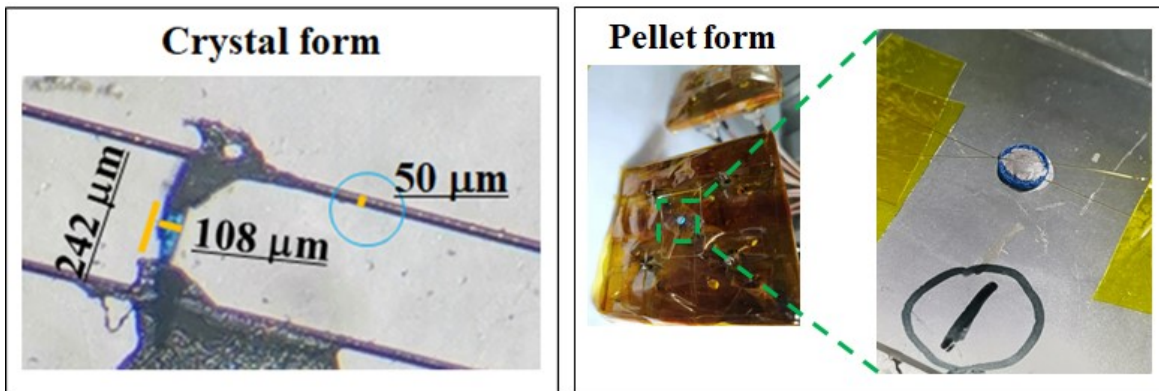


**Figure S13:** Images of proton conduction measurement setup for **IITKGP-101** in both single crystal and pellet form.

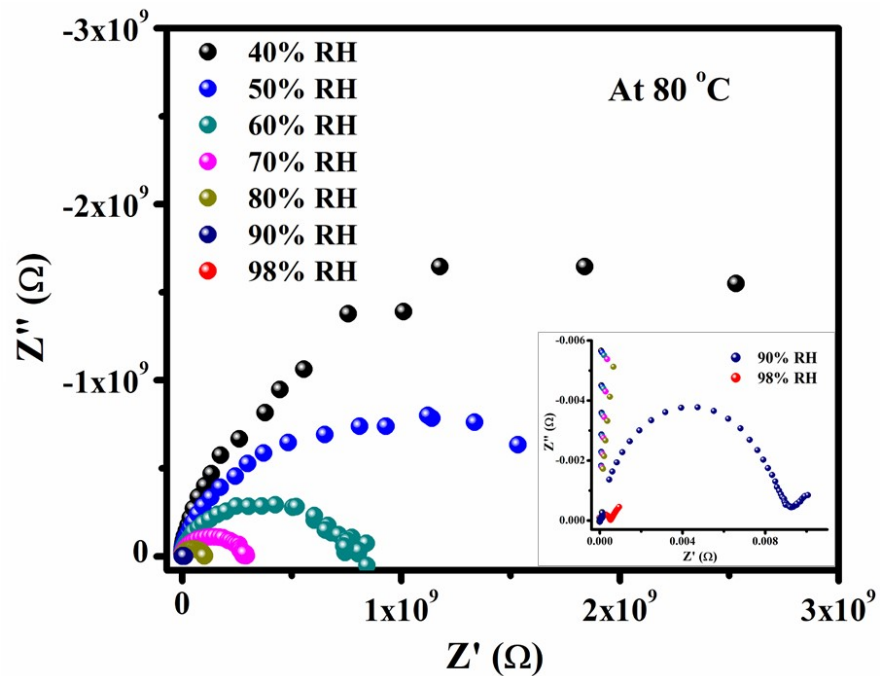


**Figure S14:** Nyquist plot of IITKGP-101 at 80 °C from 40 to 98% RH in single crystal form (inset: enlarged portion of high frequency region for clear visualization).

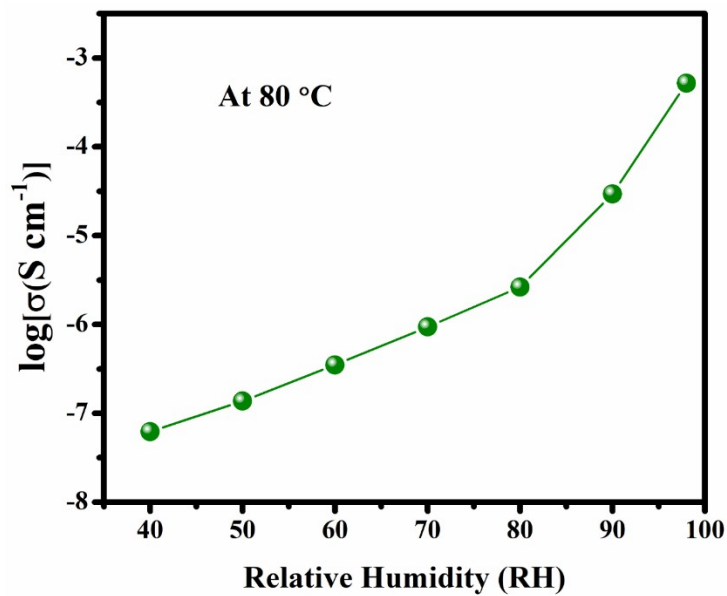


**Figure S15:** Proton conductivity vs. RH plot for IITKGP-101 in single crystal form at 80 °C.

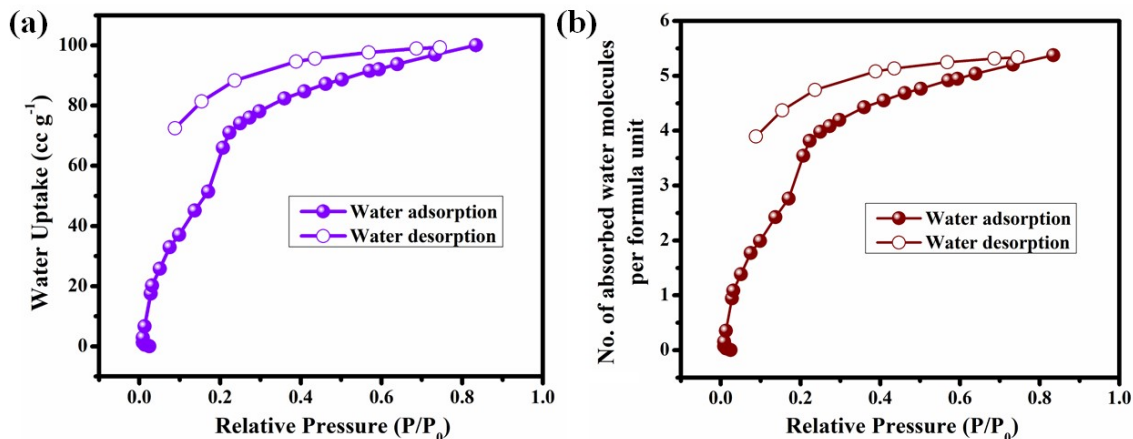


**Figure S16:** Water sorption isotherm for IITKGP-101. Closed and open symbols denote adsorption and desorption, respectively.

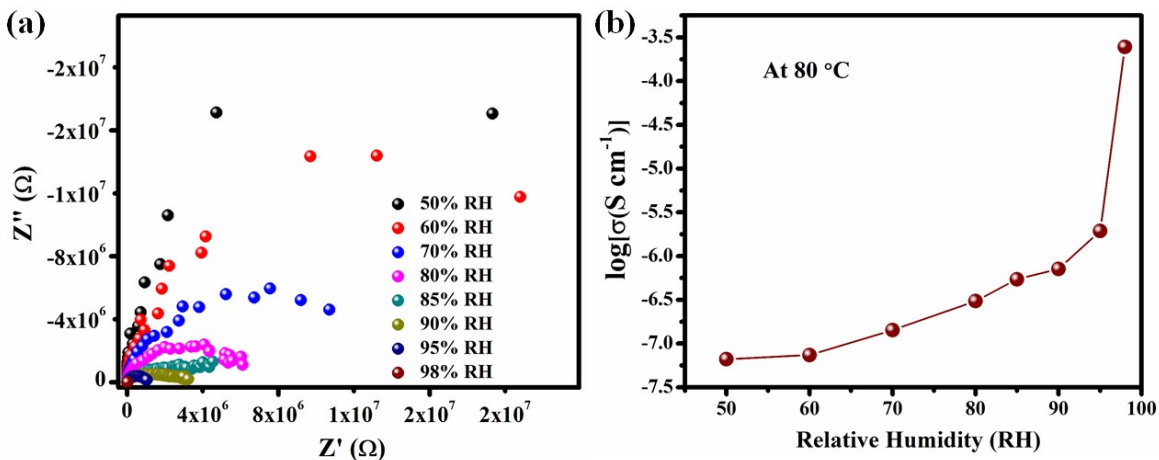


**Figure S17:** (a) Nyquist plot of IITKGP-101 at 80 °C from 40 to 98% RH in pellet form; (b) Proton conductivity vs. RH plot for IITKGP-101 in pellet form at 80 °C.

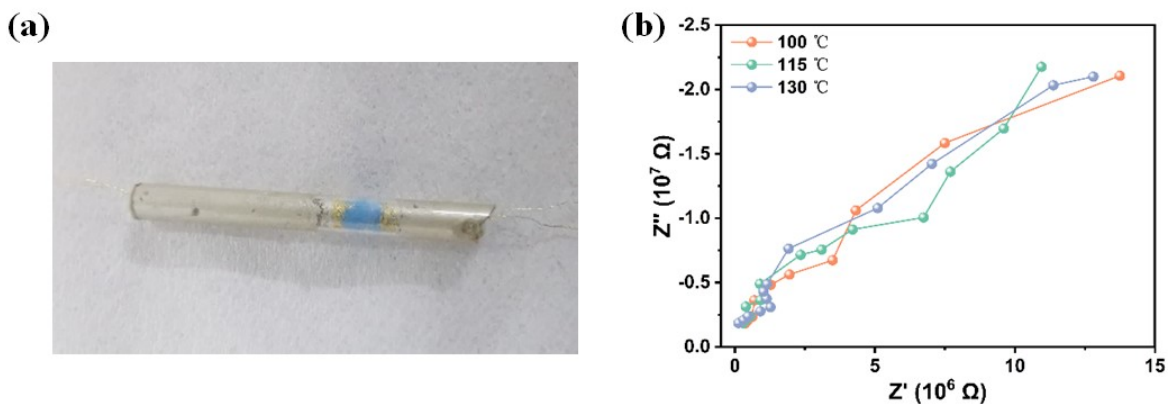


**Figure S18:** (a) Optical photograph of the IITKGP-101 device; (b) Nyquist plots of IITKGP-101 at 100, 115 and 130 °C.

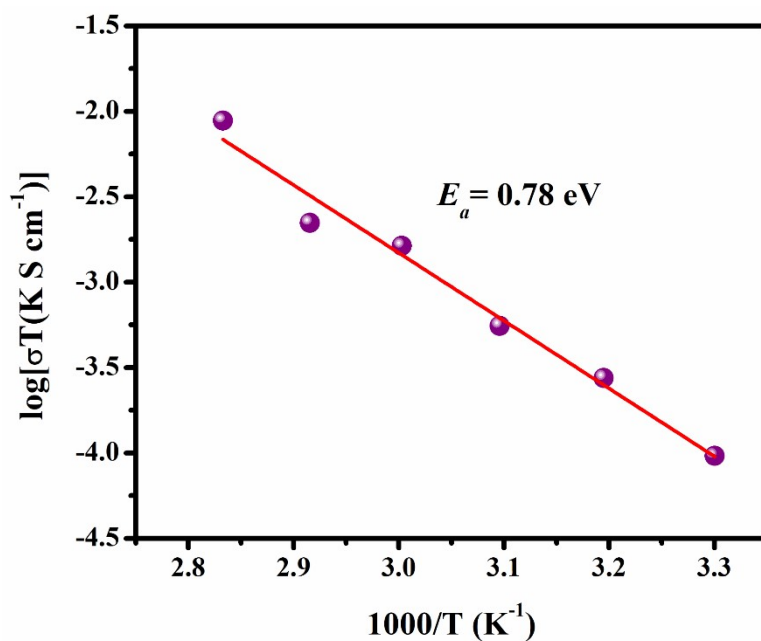


**Figure S19:** Arrhenius type plot of IITKGP-101 in the temperature range from 30 to 80 °C under 98% RH. Least square fitting is shown in the solid line.

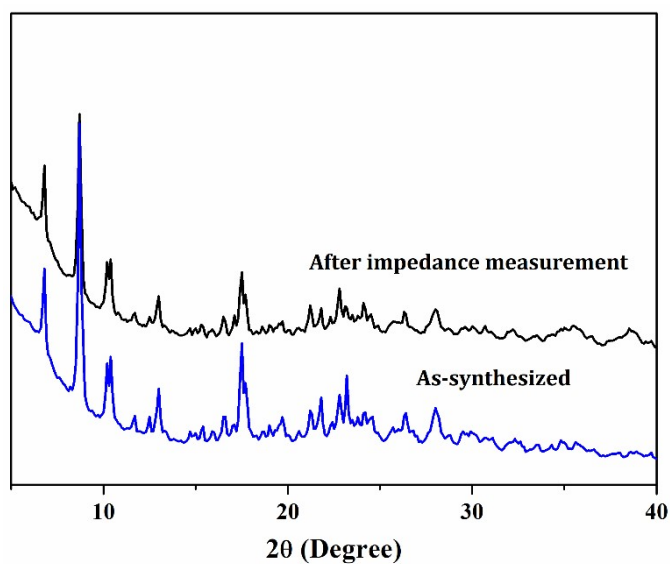


**Figure S20:** PXRD comparison for IITKGP-101 after impedance measurement.

**Table S1:** Crystal data and structure refinements for **IITKGP-101**.

Empirical formula	C <sub>40</sub> H <sub>54</sub> Cu <sub>4</sub> N <sub>4</sub> O <sub>29</sub> S <sub>4</sub>
Formula weight	1437.27
Temperature (K)	100
Radiation	Mo (k <sub>α</sub> )
Wave length (λ)	0.71073
Crystal system	Triclinic
Space group	<i>P</i> -1
<i>a</i> [Å]	13.20(3)
<i>b</i> [Å]	15.54(2)
<i>c</i> [Å]	15.89(2)
α [°]	61.15(5)
β [°]	75.86(5)
γ [°]	74.89(7)
Volume [Å <sup>3</sup> ]	2730(8)
<i>Z</i>	2
Density (calculated) [Mg m <sup>-3</sup> ]	1.749
Absorption coefficient [mm <sup>-1</sup> ]	1.785
<i>F</i> (000)	1468
Theta range for data collection	2.021 to 25.683°
Refl. used [ <i>I</i> > 2σ( <i>I</i> )]	10085
Independent reflections	8522
<i>R</i> <sub>int</sub>	0.0728
Refinement method	full-matrix least squares on <i>F</i> <sup>2</sup>
GOF	1.099
Final <i>R</i> indices [ <i>I</i> > 2σ( <i>I</i> )]	<i>R</i> <sub>1</sub> =0.1195 <i>wR</i> <sub>2</sub> =0.3215
<i>R</i> indices (all data)	<i>R</i> <sub>1</sub> =0.1334 <i>wR</i> <sub>2</sub> =0.3299
<b>CCDC</b>	<b>2220922</b>

**Table S2:** Selected Bond Distances (Å) and Bond Angles (°) in **IITKGP-101**.

Selected bond lengths [Å]

Cu1–O1	1.953(7)	Cu2–O2	1.970(8)
Cu1–O2	1.96(1)	Cu2–N3	2.04(1)
Cu1–O12	2.682(1)	Cu2–O4	2.36(1)
Cu1–N1	2.010(1)	Cu2–O5	2.00(1)
Cu1–O3	2.004(8)	Cu3–O7	1.994(1)
Cu4–O7	1.943(8)	Cu3–O6	1.953(7)
Cu4–O6	1.973(1)	Cu3–N2	2.044(1)
Cu4–O8	1.973(9)	Cu3–O10	2.395(1)
Cu4–O23	2.09(2)	Cu3–O9	1.97(1)
Cu2–O1	1.994(1)		

Selected bond angles [°]

O1–Cu1–O2	80.0(4)	O1–Cu2–O2	79.0(4)
O1–Cu1–O12	91.8(4)	O1–Cu2–N3	172.0(4)
O1–Cu1–N1	93.3(4)	O1–Cu2–O4	97.3(4)
O1–Cu1–O3	170.8(4)	O1–Cu2–O5	94.2(5)
O1–Cu1–O6	80.9(4)	O1–Cu2–O7	79.4(3)
O2–Cu1–O12	99.3(4)	O2–Cu2–N3	96.4(4)
O2–Cu1–N1	171.9(4)	O2–Cu2–O4	88.2(4)
O2–Cu1–O3	91.4(4)	O2–Cu2–O5	173.1(5)
O2–Cu1–O6	81.3(4)	O2–Cu2–O7	77.7(3)
O12–Cu1–N1	85.4(4)	N3–Cu2–O4	89.1(4)
O12–Cu1–O3	86.1(4)	N3–Cu2–O5	90.3(5)
O12–Cu1–O6	172.4(3)	N3–Cu2–O7	93.2(4)
N1–Cu1–O3	95.5(5)	O4–Cu2–O5	93.4(5)
N1–Cu1–O6	93.1(4)	O4–Cu2–O7	165.9(4)
O3–Cu1–O6	101.5(4)	O5–Cu2–O7	100.6(4)
O7–Cu4–O6	83.1(4)	O7–Cu3–O6	82.1(4)
O7–Cu4–O8	170.5(5)	O7–Cu3–N2	174.3(4)
O7–Cu4–O23	77.4(5)	O7–Cu3–O10	89.2(4)
O7–Cu4–O2	85.0(4)	O7–Cu3–O9	93.5(5)
O7–Cu4–N4	93.4(4)	O7–Cu3–O1	83.3(4)
O6–Cu4–O8	90.0(4)	O6–Cu3–N2	94.6(4)
O6–Cu4–O23	91.0(5)	O6–Cu3–O10	92.4(4)
O6–Cu4–O2	86.1(4)	O6–Cu3–O9	175.2(5)
O6–Cu4–N4	173.0(4)	O6–Cu3–O1	83.1(4)
O8–Cu4–O23	96.3(6)	N2–Cu3–O10	86.2(4)
O8–Cu4–O2	101.1(4)	N2–Cu3–O9	89.9(5)
O8–Cu4–N4	92.8(5)	N2–Cu3–O1	101.0(4)
O23–Cu4–O2	162.4(5)	O10–Cu3–O9	89.5(5)
O23–Cu4–N4	82.4(6)	O10–Cu3–O1	171.7(4)
O2–Cu4–N4	99.6(4)	O9–Cu3–O1	94.5(4)

**Table S3:** Hydrogen-bonding interactions in IITKGP-101.

<b>D–H···A</b>	<b>d(H···A)(Å)</b>	<b>D(D···A) (Å)</b>	<b>∠DHA(°)</b>
Ow1–Hw1A···O15	2.25	2.86(2)	128
Ow1–Hw1B···O21	2.07	2.79(2)	142
Ow2–Hw2B···Ow1	2.03	2.69(4)	134
O3–H3A···O11	2.53	3.304(18)	140
Ow3–Hw3A···Ow4	2.11	2.61(4)	118
Ow3–Hw3B···O6	2.22	2.85(2)	131
O3–H3B···O22	2.16	3.09(2)	173
O4–H4A···O12	2.35	2.793(18)	109
Ow4–Hw4B···O13	2.17	2.76(3)	126
O4–H4B···Ow2	1.77	2.66(3)	158
O5–H5A···O18	2.09	2.97(3)	158
Ow6–Hw6A···O17	2.00	2.65(2)	133
Ow6–Hw6B···O16	1.91	2.74(2)	165
O8–H8A···O20	2.54	3.10(2)	119
O8–H8B···O13	2.31	3.160(18)	152
O9–H9A···Ow6	2.06	2.98(2)	171
O9–H9B···O15	2.19	2.926(18)	135
O10–H10A···Ow3	2.29	3.05(3)	139
O10–H10A···O23	2.25	2.59(2)	101
O10–H10B···O16	2.26	2.873(18)	123
O23–H23A···O10	2.09	2.59(2)	113
O23–H23A···O14	1.82	2.67(2)	151
O23–H23B···O21	1.38	2.19(2)	141

**Table S4:** Non-bonding interactions in IITKGP-101.

<b>D–H···A</b>	<b>d(H···A)(Å)</b>	<b>D(D···A) (Å)</b>	<b>∠DHA(°)</b>
C1–H1A···O19	2.46	3.17(3)	134
C8–H8···O10	2.51	3.01(2)	114
C15–H15···O4	2.42	3.04(2)	124
C18–H18···O14	2.49	3.307(19)	147
C18–H18···O23	2.21	2.75(2)	117
C20–H20···O13	2.53	3.36(2)	149
C26–H26···O11	2.56	2.920(19)	104
C27–H27···O22	2.59	3.45(2)	154
C30–H30···O16	2.56	2.93(2)	104
C32–H32···O19	2.51	2.90(3)	105



**Table S5:** Temperature and humidity dependent proton conductivities of IITKGP-101 in single crystal form.

at 98% RH with varying temperatures		at 80 °C with varying relative humidity	
Temperature (°C)	$\sigma$ [S cm <sup>-1</sup> ]	RH (relative humidity)	$\sigma$ [S cm <sup>-1</sup> ]
30	$4.25 \times 10^{-5}$	40%	$6.22 \times 10^{-8}$
40	$4.16 \times 10^{-5}$	50%	$1.37 \times 10^{-7}$
50	$5.07 \times 10^{-5}$	60%	$3.50 \times 10^{-7}$
60	$5.86 \times 10^{-5}$	70%	$9.37 \times 10^{-7}$
70	$7.78 \times 10^{-5}$	80%	$2.64 \times 10^{-6}$
<b>80</b>	<b><math>5.22 \times 10^{-4}</math></b>	90%	$2.96 \times 10^{-5}$
		<b>98%</b>	<b><math>5.22 \times 10^{-4}</math></b>

**Table S6:** Temperature and humidity dependent proton conductivities of IITKGP-101 in pellet form.

at 98% RH with varying temperatures		at 80 °C with varying relative humidity	
Temperature (°C)	$\sigma$ [S cm <sup>-1</sup> ]	RH (relative humidity)	$\sigma$ [S cm <sup>-1</sup> ]
30	$3.17 \times 10^{-7}$	50%	$6.63 \times 10^{-8}$
40	$4.50 \times 10^{-7}$	60%	$7.39 \times 10^{-8}$
50	$1.17 \times 10^{-6}$	70%	$1.42 \times 10^{-7}$
60	$1.45 \times 10^{-6}$	80%	$3.06 \times 10^{-7}$
70	$6.47 \times 10^{-6}$	85%	$5.43 \times 10^{-7}$
<b>80</b>	<b><math>2.46 \times 10^{-4}</math></b>	90%	$7.14 \times 10^{-7}$
		95%	$1.93 \times 10^{-6}$
		<b>98%</b>	<b><math>2.46 \times 10^{-4}</math></b>

**Table S7:** Proton conductivity comparison of IITKGP-101 in single crystal form with reported MOFs and CPs where proton conductivity has been measured in single crystal form.

Compounds	Conductivity (S cm <sup>-1</sup> )	Conditions	$E_a$ (eV)	References
Zn(H <sub>2</sub> PO <sub>4</sub> ) <sub>2</sub> (TzH) <sub>2</sub>	$1.1 \times 10^{-4}$	130 °C	0.6	<i>J. Am. Chem. Soc.</i> <b>2012</b> , <i>134</i> , 12780
CoLa-II	$3.05 \times 10^{-4}$	25 °C, 95% RH	0.34	<i>J. Am. Chem. Soc.</i> <b>2014</b> , <i>136</i> , 9292
In(imdcH)(ox)	$1.11 \times 10^{-2}$	22.5 °C, 98.5% RH	–	<i>Chem. Mater.</i> <b>2014</b> , <i>26</i> , 2492
Eu <sub>2</sub> (CO <sub>3</sub> )(ox) <sub>2</sub>	$9.02 \times 10^{-5}$	80 °C	0.47	<i>J. Am. Chem. Soc.</i> <b>2014</b> , <i>136</i> , 12444
Fe(ox)(H <sub>2</sub> O) <sub>2</sub>	$5.7 \times 10^{-4}$	30 °C, 98% RH	0.17	<i>RSC Adv.</i> <b>2014</b> , <i>4</i> , 54382
CoCa·nH <sub>2</sub> O	$1 \times 10^{-3}$	25 °C, 95% RH	0.98	<i>Chem. Mater.</i> <b>2015</b> , <i>27</i> , 8116

CPM-103a	$5.8 \times 10^{-2}$	22.5 °C, 98.5% RH	0.66	<i>Angew. Chem. Int. Ed.</i> <b>2015</b> , <i>54</i> , 7886
CPM-103b	$4.7 \times 10^{-2}$	22.5 °C, 98.5% RH	–	
PCC-72	$1.2 \times 10^{-2}$	95 °C, 98% RH	0.23	<i>Adv. Mater.</i> <b>2016</b> , <i>28</i> , 10772
1·3H <sub>2</sub> O	$1.43 \times 10^{-3}$	80 °C, 95% RH	0.48	<i>Chem. Mater.</i> <b>2017</b> , <i>29</i> , 2321
In(5-Hsip) <sub>2</sub>	$1.25 \times 10^{-3}$	25 °C, 40% RH	0.31	<i>J. Am. Chem. Soc.</i> <b>2017</b> , <i>139</i> , 7176
Co-MOF-74	$6.1 \times 10^{-4}$	90 °C, 95% RH	0.15	<i>ACS Appl. Mater. Interfaces</i> <b>2018</b> , <i>10</i> , 35354
CFA-17	$2.1 \times 10^{-3}$	22 °C, 95% RH	0.68	<i>ACS Appl. Nano Mater.</i> <b>2019</b> , <i>2</i> , 291
Pt <sub>2</sub> (MPC) <sub>4</sub> Cl <sub>2</sub> Co (DMA)(HDMA)·guest	$2.2 \times 10^{-2}$	60 °C, 95% RH	0.33	<i>JACS Au</i> <b>2022</b> , <i>2</i> , 109–115
IITKGP-101	$5.2 \times 10^{-4}$	80 °C, 98% RH	0.78	<b>This Work</b>

**Table S8:** Proton conductivity comparison of **IITKGP-101** in pellet form with so far reported MOFs and CPs in which coordinated water act as *sole* intrinsic proton sources.

Compounds	Conductivity (S cm <sup>-1</sup> )	Conditions	$E_a$ (eV)	References
Mg-OBA	$1.27 \times 10^{-2}$	80 °C, 95% RH	0.13	<i>ACS Materials Lett.</i> <b>2020</b> , <i>2</i> , 1343
Ca-BTC-H <sub>2</sub> O	$1.2 \times 10^{-4}$	25 °C, 98% RH	0.18	<i>Chem. Commun.</i> <b>2012</b> , <i>48</i> , 8829
Ca-BTC-DMF	$4.8 \times 10^{-5}$	25 °C, 98% RH	0.32	
Ca-BTC-DMA	$2.0 \times 10^{-5}$	25 °C, 98% RH	0.40	
Eu-TTHA	$3.5 \times 10^{-3}$	80 °C, 98% RH	0.44	<i>RSC Adv.</i> <b>2021</b> , <i>11</i> , 11495
MOF 1	$1.1 \times 10^{-4}$	100 °C, 98% RH	0.38	<i>J Solid State Chem.</i> <b>2022</b> , <i>307</i> , 122874
MOF 2	$1.44 \times 10^{-4}$	100 °C, 98% RH	0.32	
Ni-MOF-74	$1.4 \times 10^{-4}$	80 °C, 95% RH	–	<i>Angew. Chem. Int. Ed.</i> <b>2014</b> , <i>53</i> , 8383
HKUST-1	$1.5 \times 10^{-5}$	RT	–	<i>J. Am. Chem. Soc.</i> <b>2012</b> , <i>134</i> , 51
Tb-TTHA	$2.57 \times 10^{-2}$	60 °C, 98% RH	0.68	<i>Chem. Commun.</i> <b>2019</b> , <i>55</i> , 1762
Fe(ox)	$1.3 \times 10^{-3}$	25 °C, 98% RH	0.37	<i>J. Am. Chem. Soc.</i> <b>2009</b> , <i>131</i> , 3144
Co-fdc	$4.85 \times 10^{-3}$	80 °C, 98% RH	0.4	<i>Angew. Chem. Int. Ed.</i> <b>2018</b> , <i>57</i> , 6662
Co-tri	$1.49 \times 10^{-2}$	80 °C, 98% RH	0.4	
Co-tetra	$4.15 \times 10^{-2}$	80 °C, 98% RH	0.29	
PCM-1	$1.85 \times 10^{-2}$	80 °C, 98% RH	0.38	<i>J. Mater. Chem. A</i> <b>2020</b> , <i>8</i> , 7847
Mg <sub>2</sub> (dstp)	$1.3 \times 10^{-4}$	80 °C, 50% RH	0.19	<i>Bull. Korean Chem. Soc.</i> <b>2021</b> , <i>42</i> , 322
IITKGP-101	$2.45 \times 10^{-4}$	80 °C, 98% RH	0.78	<b>This Work</b>

## References:

1. Sheldrick, G. M. Siemens Area Correction Absorption Correction Program; University of Göttingen: Göttingen, Germany, **1994**.
2. Farrugia; L. J., WinGx suite for small-molecule single crystal crystallography. *J. Appl. Crystallogr.* **1999**, *32*, 837.
3. SAINT+, 6.02ed, Bruker AXS, Madison, WI, **1999**,
4. XPREP, 5.1 ed. Siemens Industrial Automation Inc., Madison, WI, **1995**,
5. Sheldrick; G. M., SHELXL-97 Program for Crystal Structure Solution and Refinement; University of Göttingen: Göttingen, Germany, **1997**.
6. G. M. Sheldrick, Crystal Structure Refinement with SHELXL. *Acta Cryst C* **2015**, *71*, 3–8.